ORIGINAL PAPER

Conceptual analysis for a technology demonstration mission of the ion beam shepherds

Ricardo Colpari[1] · Niki Sajjad[2] · Anoop Kiran[3] · Moitrayee Chakraborty[4] · Vishal Tripathi[5] · Prerna Baranwal[6] · Bhavyashree Janardhana[4] · Daria Stepanova[7] · Daniel Wischert[8]

Abstract

Low Earth Orbit is exceptionally constrained by the increasing number of satellites, increasing collision risks that might lead to significant losses in technological advancement. Hence, it is imperative to develop techniques such as Active Debris Removal (ADR) to preserve the usability of the space environment surrounding Earth. A promising ADR technique consistent with contactless operation constraints, which is undergoing rapid development, is known as the Ion Beam Shepherd (IBS). This revolves around using a highly collimated ion beam to continuously exert a force at a close range on the debris to achieve a highly controlled deorbiting. However, to date, no demonstration mission has proven this concept in space. This paper presents a survey of the main research works on the subject of IBS ADR missions along with multiple comparative analyses between alternative architectures for an in-orbit demonstration mission that could potentially increase the Technology Readiness Level (TRL) of IBS capabilities for small satellites in LEO. Particular attention is given to the mission's critical elements, such as state-of-the-art electric propulsion, techniques for collision avoidance, methods for reconstructing the dynamics of non-cooperative targets, and hazardous effects connected to IBS. The most critical risks are investigated in this paper and discussed in detail. Impulse transfer misalignment resulting in tumbling of the target, contamination risk, problems with acquiring the target based on the visual sensor inaccuracy, attitude control error in the approaching phase, and electric propulsion reliability are studied here from different angles.

Keywords Space debris removal · Active debris removal · Ion beam shepherd · In-orbit demonstration · Space rendezvous · Electric propulsion

✉ Ricardo Colpari
colpari@lpp.polytechnique.fr

Niki Sajjad
niki.sadjad@email.kntu.ac.ir

Anoop Kiran
anoopkir@buffalo.edu

Moitrayee Chakraborty
m.chakraborty@campus.tu-berlin.de

Vishal Tripathi
vishalwisdom@gmail.com

Prerna Baranwal
f2016568@pilani.bits-pilani.ac.in

Bhavyashree Janardhana
jbhavya.shree@gmail.com

Daria Stepanova
daria.stepanova@skolkovotech.ru

Daniel Wischert
daniel.wischert@spacegeneration.org

[1] Ecole Polytechnique, Palaiseau, France

[2] Space Research Laboratory, K. N. Toosi University of Technology, Tehran, Iran

[3] University at Buffalo, The State University of New York, Buffalo, NY, USA

[4] Technische Universität Berlin, Berlin, Germany

[5] Space Generation Advisory Council, Chennai, India

[6] Department of Electrical and Electronics/Instrumentation and Department of Mathematics, Birla Institute of Technology and Science (BITS), Pilani, Rajasthan 333031, India

[7] German Orbital Systems GmbH, Manfred-Fuchs-Platz 2-4, 28359 Bremen, Germany

[8] Space Generation Advisory Council (SGAC), c/o European Space Policy Institute, Schwarzenbergplatz 6, 1030 Vienna, Austria

Abbreviations

ADR	Active debris removal
CW	Clohessy–Wiltshire equations
DST	Double-sided thruster
EP	Electrical propulsion
GEO	Geostationary ORBIT
GIT	Gridded ion thrusters
GNC	Guidance, navigation, and control
HET	Hall effect thrusters
IBS	Ion beam shepherd
Isp	Specific impulse
IC	Impulse compensation
ICT	Impulse compensation thruster
IT	Impulse transfer
ITT	Impulse transfer thruster
LEO	Low earth orbit
PD	Proportional derivative
RCS	Reaction control system
SDO	Space debris object
SS	Space shepherd
TRL	Technology readiness level

1 Introduction

For several years, the problem of ever-increasing numbers of Space Debris Objects (SDO) in orbits around the earth has come to the attention of scientists and space policy decision-makers. Earth-orbiting objects, large enough to be tracked, have been surveyed for possible systematic debris removal, the reason for this is that collisions between large objects in space will slowly but surely increase the number of dangerous debris fragments. These in turn will produce more debris and so on in a chain reaction. Objects in low-altitude orbits (below ~ 500 km) are affected by atmospheric drag. This lowers their orbit until they re-enter the atmosphere and are thus naturally removed from orbit. The lower the orbit the faster it decays. However, for satellites with higher attitudes this is not the case: based upon the statistical collision studies, it was determined that objects in orbits approximately 1000 km above the Earth's surface area are at the greatest collisional risk.

Looking at the huge amount of space debris already in existence, Active methods for Debris Removal (ADR) and on-orbit servicing of satellites along with the compliance of mission disposal guidelines for new space missions have been considered effective in stabilizing and eventually minimizing the debris growth and ensuring long-term space sustainability. A large number of various active debris removal methods have been proposed, designed and developed, each having their own share of advantages and disadvantages. The most promising and competitive contact-based methods include using robotic manipulators, tethers, nets, and harpoons, whereas the contact-less methods are laser-based, ion-beam shepherd ADR methods.

Using a robotic arm to capture the target has been one of the most talked about and proposed method, but it would not be suitable for capturing irregular-shaped fast-spinning debris with no specific capture points [1, 2], until 2021 numerical simulations demonstrated that this shortcoming could be overcoming by a combination of compliant clamping control and adaptive backstepping-based Trajectory Tracking Control, and propellant consumption could be reduced. However, it would increase the complexity of the mission and the mass of the satellite [3]. Another contact-based promising ADR technology for a long time has been the use of the Electrodynamic tether, which works on the principle of the drag thrust produced by the flow of electrons through the length of the tether in the presence of the Earth's magnetic field that helps de-orbit the system. Even though this technology would be simple, lightweight, and propellant-less, there are certain disadvantages and risks involved that cannot be eliminated such as very low Technology Readiness Level (TRL), possibility of severing, risk of collision with operation satellites, additional tension control for tumbling debris and tug safety [4–6]. In lieu of using only a tether, another integrated technology emerged, a tethered net could also be suitable for non-cooperative spinning objects. In this case, the net would be mounted on a chaser satellite which when ejected towards the target debris entangles and wraps around it, then deorbiting by towing the tethered object to a lower altitude orbit. However, this technology has a low technical maturity and could involve high risk in the net closing mechanism [7–9]. Similarly, the usage of harpoon along with a tether as an ADR method has also been proposed in many of the research articles, involving a set of barbs shot from a chaser satellite by means of a tether for penetrating the debris surface. But it could generate more and more smaller debris particles on colliding with the target, and it cannot capture targets with a high tumbling rate, causing it to rebound off its surface [7, 10, 11].

Contact-less methods of orbital debris removal would have the obvious advantage of not risking more debris creation due to violent collisions. Among these contact-less methods, ground-based and spaceborne laser-based technology have been some of the renowned ADR technologies [12, 13]. High-powered pulsed-laser systems shoot onto target debris to reduce its velocity and eventually lower its altitude. However, the risk of new debris formation is higher in the case of these systems. A ground-based laser system would require to bridge a huge distance to focus a beam on debris with a very small radius. Furthermore, it would require a large beam director mirror to obtain high power density to produce an impactful impulse on the debris target, thus increasing cost and complexity. A promising, talked-about ADR technology is the Ion-Beam Shepherd (IBS) method,

aspects of which will be described in detail throughout this article. Some of the major motivations in the selection of this method for technology demonstration are; its contactless approach; working concept irrespective of target shape, material or rotation; reusability feature until fuel depletion to focus on multi-target removal, high specific impulse due to its high TRL electric-propulsion technology [14].

There are few active space debris removal missions that have already been deployed in space successfully. The first one is the RemoveDebris which has been a low-cost mission performing ADR using a combination of various technologies mentioned above: a net, harpoon, a vision-based navigation system and finally a drag sail. This mission involved experiments that helped mature net and harpoon technologies in space which had very low TRLs [15, 16]. The world's first commercial ADR demonstration was launched on 22nd March 2021, named as End-of-Life Services by Astroscale-demonstration (ELSA-d) [17]. This mission includes a servicer smallsat responsible for performing far and short-range rendezvous and proximity operations, client search and inspection, a magnetic capture system with a docking mechanism. There are a few more ADR demonstration missions like ETS-VII, ClearSpace-1 and ANDROID that have been responsible for performing technological testing and verification of activities required in ADR [3, 18–20].

This paper primarily gives a detailed description of various design aspects in developing a demonstration technology based on an ion-beam shepherd concept, structured as follows. This work only considers a single target debris removal, since this is a technology demonstration mission, and involves the least amount of orbital transfers to be analyzed, allowing a more in-depth study of the deorbiting maneuver. Section 2 begins with an introduction of the IBS concept, followed by Sect. 3 which describes a mission plan proposal that encompasses various relevant phases such as identifying the target (debris) orbit, approach and far-range rendezvous, close-range rendezvous and inspection and deorbiting. The close-range rendezvous section

is further explained keeping in mind a lot of important factors that include guidance, safe-distance trajectories, target inspection, navigation, pose estimation and stability and control of the deorbiting phase. Section 4 further goes on to discuss the proposed architecture for the mission that involves both the platform and the propulsion system. Section 5 contains discussions about some additional considerations and risks to give a better understanding of the entirety of this demonstration mission. Finally, Sect. 6 draws conclusions.

2 The Ion Beam Shepherd

The Ion Beam Shepherd (IBS) is a contactless space debris removal system, initially, this concept was formally explored in [21] by proposing analytical and control models. In the IBS the debris orbital motion is actively controlled by exploiting the momentum transmitted by a collimated beam of quasi-neutral plasma impinging against its surface as depicted in Fig. 1. The beam can be generated with advanced ion engines from a shepherd spacecraft orbiting nearby. This spacecraft, placed at a certain distance from the object, would use a state-of-the-art ion thruster pointed towards the debris, called the Impulse Transfer Thruster (ITT), as well as a second propulsion system to compensate for the beam reaction to keep a constant distance between the debris and the shepherd satellite throughout the deorbiting process, the Impulse Compensation Thruster (ICT).

Since the concept was formally presented, there have been multiple research groups working in different aspects of the mission, overcoming some of the limitations. This work is going to propose an updated review of different works and analyze the feasibility of a demonstration mission of the IBS using current small satellite capabilities.

Fig. 1 Schematic of ion beam shepherd satellite deorbiting space debris
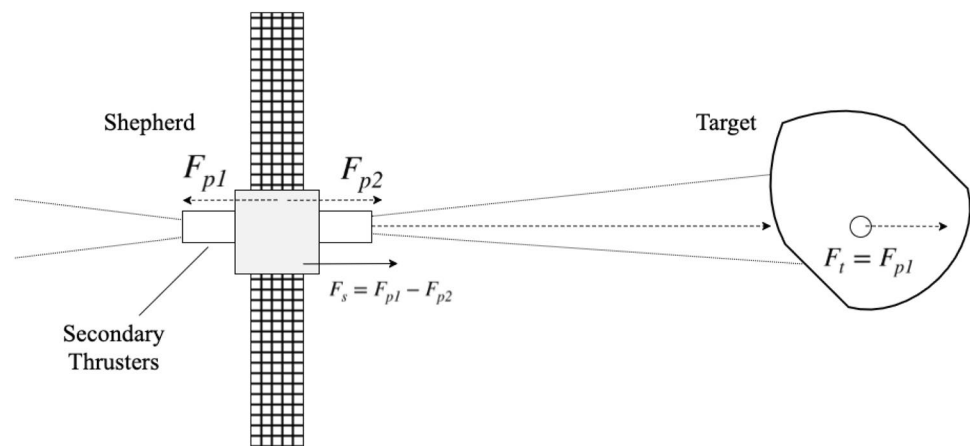
3 Mission proposal

This section reviews the mission operation phases and parameters required for a successful design of an IBS mission.

3.1 Mission operations concept

The concept of operations of this mission consists to launch and to commission the satellites to the selected inclinations, the schematic can be seen in Fig. 2.

To perform the rendezvous and inspection for this mission, different phases have been identified:

- Identify the Target's orbit
- Approach and far-range rendezvous
- Close range rendezvous and inspection
- Deorbiting

The following subsections will detail each phase, many of these phases are common to any ADR mission, therefore, the detail will be stressed only in the phases that are more specifically related to an IBS mission.

3.2 Identify the target's orbit

The starting point assumption is that the orbit of the target is given and serves as an input to the problem statement. While there is a significant amount of satellites in GEO orbit, a demonstration mission would be costlier and more difficult to realize there, therefore, the focus of this work will be done solely in LEO. Most satellites are in LEO and that is where the most amount of debris formation might take place. Databases of current operational satellites in orbit can be found in [22], the list can be exported and sorted according to different parameters, to study possible target orbits, the list was sorted according to the number of satellites by inclination and the number of satellites by altitude. The distribution can be seen in Fig. 3. Out of all these satellites, most of them
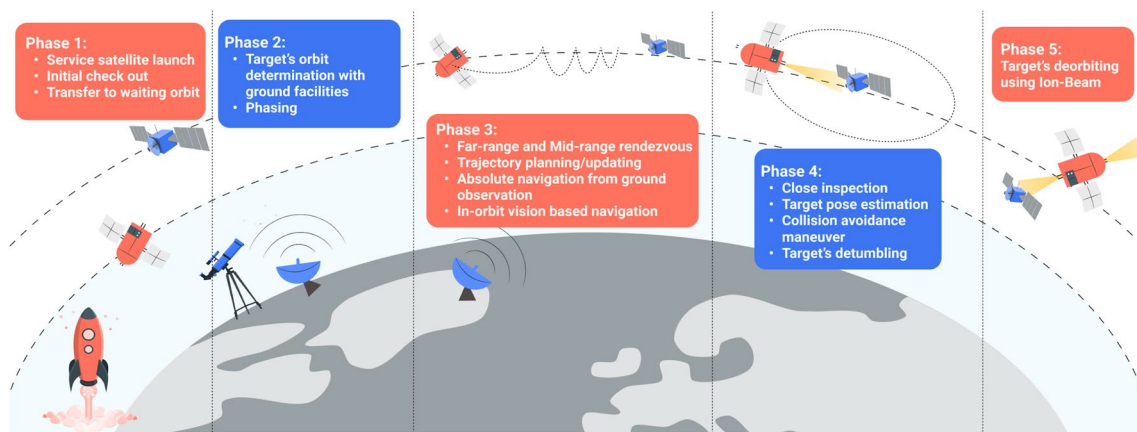
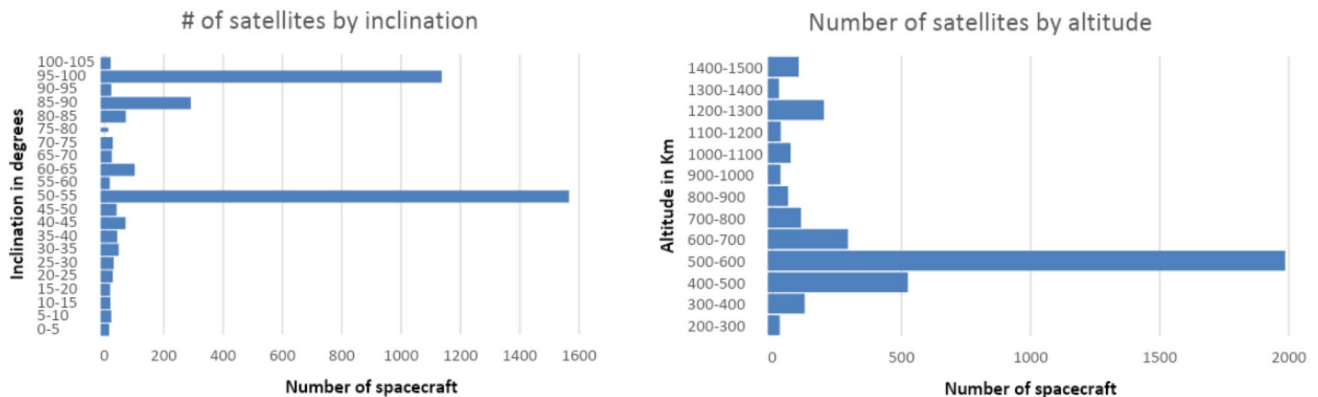

Fig. 2 ConOps of an IBS mission

Fig. 3 Number of satellites by inclination and altitude

are in Polar orbit, predominantly around the inclination of 90–98 deg. Regarding the altitude, the greatest concentration of debris is found between 800 and 850 km in orbit [22]. A full-fledged IBS mission shall possess "multi-mission" capabilities, that is, to be able to shepherd several SDO during its lifetime, therefore, the limited mission duration and a Δv budget are imposed as constraints. Nevertheless, in this review of different works, only the case for a demonstration mission of one target will be analyzed. The case for a single target is considered as it is simpler to analyze as compared to multi-target rendezvous. Further analysis needs to be carried out if it is necessary to utilize the same operations procedure for multiple targets.

3.3 Approach and far-rendezvous

After launch and commissioning, the IBS first reaches a waiting orbit, typically set at low altitudes to facilitate the phasing; when an SDO is identified to start the mission, the orbital parameters of the target will be provided by a ground tracking station. This phase of absolute navigation requires Two-line Elements (TLE) data, this allows the Shepherd Satellite (SS) to start the approach and phasing with the target and position itself close to it, the endpoint of phasing is often called the 'initial aim point'. Locating this point behind and slightly below the target is the most convenient solution, as the natural drift will move the inspector slowly towards the target without additional propulsion maneuvers. During such drift, residual errors after the last maneuvers in terms of height, eccentricity, and out-of-plane errors can be corrected.

Then the phase of far rendezvous starts, it is the start of the relative navigation phase, to determine the relative state between the chaser and the target. To study the relative orbit dynamics, the main equations to be used are the Clohessy–Wiltshire (CW) equations [23], these equations, Eq. (1) and Eq. (2), will be used to design the guidance law in the depicted reference frame in Fig. 4., as well as the control during the deorbiting phase.

$$\begin{cases} \ddot{x} = 3n^2x + 2n\dot{y} \\ \ddot{y} = -2n\dot{x} \\ \ddot{z} = -n^2x \end{cases} \tag{1}$$

where $n = \sqrt{\frac{\mu}{a_t^3}}$.

These equations have a closed-form solution as follows:

$$\begin{cases} x(t) = \frac{\dot{x}_0}{n}\sin(nt) - \left(3x_0 + \frac{2\dot{y}_0}{n}\right)\cos(nt) + \left(4x_0 + \frac{2\dot{y}_0}{n}\right) \\ y(t) = \left(6x_0 + \frac{4\dot{y}_0}{n}\right)\sin(nt) + 2\frac{\dot{x}_0}{n}\cos(nt) - \left(6nx_0 + 3\dot{y}_0\right)t + \left(y_0 - 2\frac{\dot{x}_0}{n}\right) \\ z(t) = z_0\cos(nt) + \frac{\dot{z}_0}{n}\sin(nt) \end{cases} \tag{2}$$
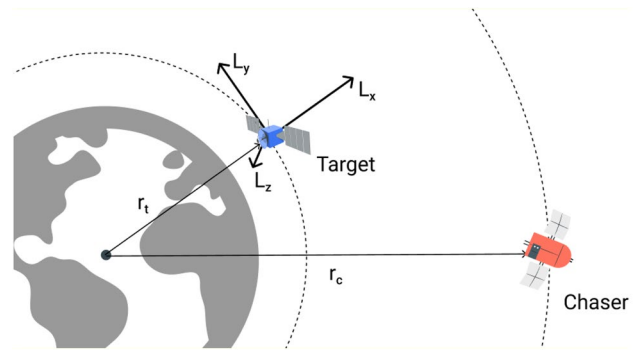

Fig. 4 Reference frame for CW equations

where x_0, y_0, z_0, $\dot{x}_0$, $\dot{y}_0$, $\dot{z}_0$ are initial values of position and velocity coordinates. These equations are going to be used not only in the Far Rendezvous but mostly in the Close Rendezvous phase of the mission.

During the first approach, vision-based navigation will get the relative attitude and Lidar is used for ranging between the inspector and the target, this one is also important to maintain a safe distance, the final point of the rendezvous is at a distance of fewer than 500 m in the direction of velocity for the CW relative frame (V-bar) to the target.

3.4 Close rendezvous and target's characterization

Uncooperative objects with unknown physical properties pose many technical difficulties and not one method is suitable to deal with all types of scenarios. Obtaining accurate pose information of uncooperative objects still remains a difficult task and selecting the correct sensors and estimation algorithms are critical. Moreover, trajectory planning is a prerequisite for precise demonstration of navigation, pose estimation, and execution of fault-tolerant formation flying maneuvers between the chaser and the target in the close-range phase.

3.4.1 Guidance

In close-proximity flight, the capability of reducing the collision risk, as well as of determining with high accuracy the target relative position and attitude, has a significant impact on the control system design and required control power and, consequently, on mission and satellite costs. Therefore, the adoption of a suitable guidance solution, in terms of relative trajectory design, can play a key role.

Every servicing mission needs two essential steps for guidance to be implemented. First, defining the form of trajectory and boundary conditions, and second, trajectory updating and optimization. The first step determines

in which form the chaser will follow the target to reach a close distance and what constraints should be considered. Mission constraints make a huge difference between these trajectories and let mission designers prioritize one method over another. Collision avoidance, thruster saturation, velocity boundary conditions, plume impingement avoidance and real-time generation of trajectories with low computational expense are the most important constraints of this phase.

The second step of guidance is computing onboard a feasible trajectory from the actual configuration of the chaser spacecraft to the desired point. The computation of the trajectory is executed in real-time by the path planner algorithm. This algorithm should cover both translational and rotational trajectories of the chaser for the case of the 6 Degrees of Freedom dynamic. The path planning algorithm must be able to enforce path constraints such as sensor pointing, mission time limits, thrust budget, and collision avoidance. Since the thrust is a crucial factor for the satellite, low-thrust/thrust-optimal trajectories are desired.

The following issues will be discussed in this part:

- Optimization of safe distance maneuver
- Inspection trajectory design
- Collision avoidance maneuver with a failure tolerant algorithm

3.4.1.1 Safe distance trajectory When a spacecraft conducts a proximity operation, it is important that the chaser satellite remains near the target without getting too close to cause a collision. Considering the Clohessy–Wiltshire (CW) frame, the target satellite is at the origin as in Fig. 5. The safety requirement will be presented as a constraint on the state of the chaser spacecraft:

$$r\_min \leq r \leq r\_max \tag{3}$$

When the state r is described as $r = (x, y, z, \dot{x}, \dot{y}, \dot{z})^T$

Satisfying all the constraints is quite challenging and the verification process has its own challenges due to the following reasons:

1. The target spacecraft often has its own control policy, which may not be known ahead of time (or at all). The safety verification process should be robust to some bounded maneuvering by the target satellite.
2. The safety verification process should allow maximum flexibility in designing the controller, As designing a spacecraft controller is challenging for this phase.

Some existing guidance strategies that have been proposed for autonomous rendezvous and proximity operations to an uncontrolled target in the last decade are known as:

- Glideslope Algorithm: It is used inherently to provide guidance for spacecraft to perform flybys, and depart from the target vehicle in a circular orbit, enabling the spacecraft to circumnavigate the target spacecraft in any plane. It calculates the velocity corrections required to follow a predefined linear velocity profile for a mission, with a certain set frequency. The algorithm blends path planning and velocity control algorithms, enabling autonomous docking to a cooperative tumbling target [24].
- Mixed Integer Linear Programming: It seeks to alter the objective function by maximizing or minimizing the combination of parameters, variables and several constraints on the variable. It is implemented to attain minimum-fuel, fixed-time maneuvers coupled with inherent constraints due to collision avoidance. The fuel expenditure is minimized by optimizing the values of the controls in each interval. The MILP-based path planner has two important strengths: first, it provides fuel-optimal trajectories and second, path constraints can be enforced, including plume impingement and passive safety under thruster failures toward the end of the trajectory [25].
- Model Predictive Control (MPC): It is developed to solve constrained trajectory optimization problems when executed in a closed loop for the entire maneuver. The MPC employs the dynamics model of the system to sample the state vector for a relatively short time horizon in the future starting from the current instant. The discretized controls and states are subsequently used to formulate a constrained optimization problem, which is solved using common numerical techniques [26].

Fig. 5 The chaser satellite safe distance
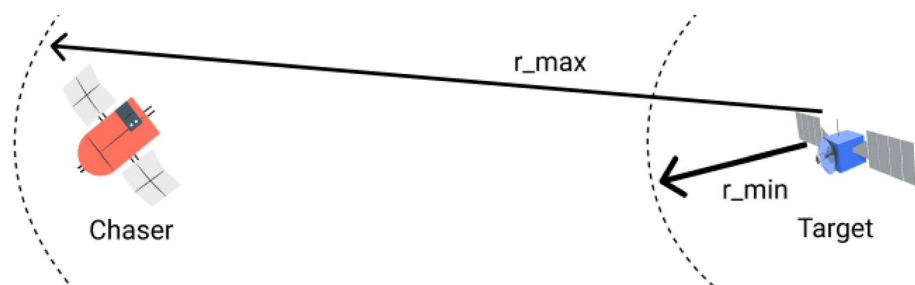
- Rapidly exploring Random Tree: It searches for high-dimensional spaces that exist in the samples drawn randomly from the search space. The space-filling tree grows incrementally towards unsearched areas that have been determined based on the problem at hand. Starting from the current position of the vehicle, the algorithm randomly builds a space-filling tree of the 3D space. The vehicle trajectory is obtained using the consecutive nodes of the randomized data structure that minimize a certain performance index while respecting path constraints [27].

- Inverse Dynamics in the Virtual Domain (IDVD): It imposes a trajectory of the vehicle using a set of interpolating functions defined in the virtual domain of time. Upon inverting the dynamics model of the system, state variables, controls, path constraints and performance index are expressed as nonlinear functions in the virtual domain of the parameterized trajectory and its derivatives. By linking the known endpoint conditions such as the position and velocity with the functions' polynomial coefficients, the boundary conditions of the trajectory are enforced [28].

- Quasi-analytical guidance algorithm: It helps achieve the capability of rendezvous and dock in the presence of tumbling objects. Similar to other guidance and control algorithms, it seeks to allow for spacecraft to capture an uncooperative and tumbling object under constraints that the spacecraft is exposed to, including speed bounds, collision avoidance etc. It also finds numerous applications in the areas of in-space assembly, satellite servicing, and active debris removal (ADR) [29].

Recently, some methods showed strengths over other algorithms. The trajectory should be easily stored on board and be a low thrust solution. The trajectory should also be able to be rapidly reshaped using the coefficients previously optimized and the most current data from the navigation system. MPC [30], IDVD [31], and Quasi-analytical solutions [32] are growing rapidly due to their flexibility and great optimization results. We follow the MPC approach as it is a method for both control and trajectory optimization, it is well-studied, nonlinear optimization is available, and constrained maneuvers (like low-thrust maneuvers) are already performed using this method. Moreover, MPC enables online optimization for real-time operations of collision avoidance.

3.4.1.2 Target inspection Optical inspection of the target is required at close ranges during autonomous rendezvous. The target inspection and imaging phase is the vital part and the ultimate objective of the mission. The relative motion of the chaser should be exploited to fully characterize the target in the inspection phase. The trajectory must be passively safe, hence natural motion shall be explored to achieve relative orbits, which do not threaten the safety of this phase. The criteria to select the relative trajectory are (1) passive safety compliance (2) invariance to target geometry and attitude motion (3) optimal sun-phase angle and avoidance of Field Of View (FOV) occultation [33].

Three different scenarios have been discussed recently. One of the very common approaches is to exploit the in-plane motion of the chaser around the target which is shown in Fig. 6(a). This is an easy trajectory to be designed. However, as the target attitude motion is unknown, this trajectory, which is limited to one specific plane, is risky for complete imaging and covering the target from different angles. Moreover, the relative orbit crosses the V-bar twice in its natural motion which means that the chaser intersects the target orbital path. The along-track orbit determination is more uncertain with respect to the radial and cross-track components because of the coupling between the semi-major axis and orbital period. This problem can be solved by inserting an across-track component that results in an out-of-plane trajectory shown in Fig. 6(b). This trajectory guarantees full coverage of the target and reduces the risk of collision with the target. It also foresees passive trajectories that drift along the v-bar coupled with a cross-track motion component. As a disadvantage, the FOV acquisition is poor, Earth is in the FOV when the trajectory is centered on the target, and target attitude motion still affects the trajectory.
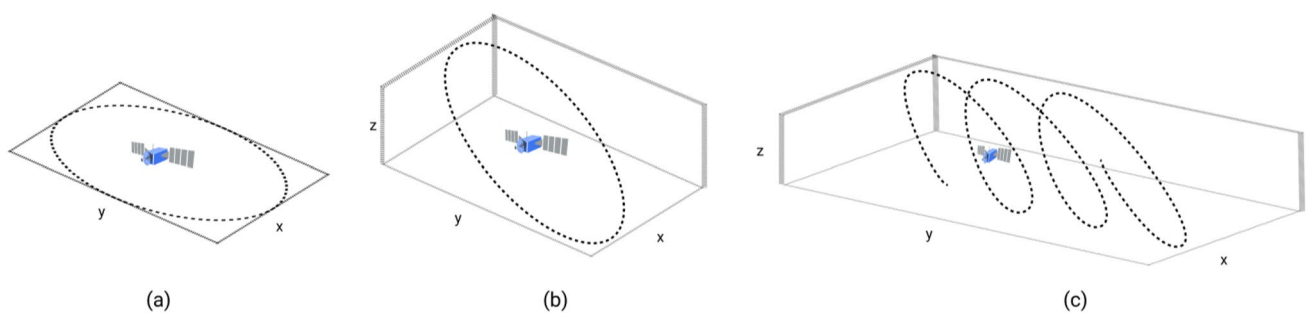

Fig. 6 Relative motion in target inspection phase, **a** in-plane, **b** out-of-plane, **c** drifting

Considering the state vector defined as: $(x(t)y(t)z(t)\dot{x}(t)\dot{y}(t)\dot{z}(t))^T$

The CW equations state transition matrix is derived as:

$$\begin{pmatrix} x(t) \\ y(t) \\ z(t) \\ \dot{x}(t) \\ \dot{y}(t) \\ \dot{z}(t) \end{pmatrix} = \begin{pmatrix} 4-3\cos nt & 0 & 0 & \frac{1}{n}\sin nt & \frac{2}{n}(1-\cos nt) & 0 \\ 6(\sin nt - nt) & 1 & 0 & -\frac{2}{n}(1-\cos nt) & \frac{1}{n}(4\sin nt - 3nt) & 0 \\ 0 & 0 & \cos nt & 0 & 0 & \frac{1}{n}\sin nt \\ 3n\sin nt & 0 & 0 & \cos nt & 2\sin nt & 0 \\ -6n(1-\cos nt) & 0 & 0 & -2\sin nt & 4\cos nt - 3 & 0 \\ 0 & 0 & -n\sin nt & 0 & 0 & \cos nt \end{pmatrix} \begin{pmatrix} x_0 \\ y_0 \\ z_0 \\ \dot{x}_0 \\ \dot{y}_0 \\ \dot{z}_0 \end{pmatrix} \quad (4)$$

The term $(y_0 - \frac{2}{n}\dot{x}_0)$ produces a constant offset in y(t) and $(6nx_0 + 3\dot{y}_0)t$ makes y(t) an increasing function. Hence, to have a no-offset condition, the first term should be eliminated. Therefore, the initial condition would be:

$$y_0 = \frac{2}{n}\dot{x}_0 \quad (5)$$

To achieve the non-drifting condition, the initial condition should remove the second term and thus, it should be chosen as:

$$\dot{y}_0 = -2nx_0 \quad (6)$$

So, the solution for the in-plane motion of the chaser satellite will be written as:

$$\begin{cases} x(t) = -A_0 cos(nt + \alpha) \\ y(t) = 2A_0 sin(nt + \alpha) \end{cases} \quad (7)$$

The out-of-plane motion is decoupled from the in-plane motion and its solution takes the shape of a simple harmonic oscillator:

$$z(t) = B_0 sin(nt + \beta) \quad (8)$$

where amplitudes A_0, B_0 and phase angles α, β are constants dependent on the initial conditions.

Using the above equations we can design different trajectories. Hence, the trajectory that completes target coverage regardless of its attitude motion, considers collision avoidance motion, which is robust and can be applied to different targets and has a high Field Of View acquisition would be selected. This trajectory is a drifting out-of-plane trajectory, which gives the flight profile that includes a wide range of relative attitude and position in the region around the target (meaning different sun-phase angles and line-of-sight) during the inspection phase.

The relative orbital transfer between hold orbits and inspection orbits is performed using the MPC method with thrust and duration constraints derived from the electric propulsion system. The algorithm allows a safe reconfiguration and results in a specific maximum Δv per maneuver considering power constraint and maximum thrusting window.

3.4.2 Navigation

Navigation refers to the determination, at a given time, of the vehicle's location and velocity (the "state vector") as well as its attitude. This capability is critical to autonomously rendezvous to noncooperative space targets. Therefore, it is a common challenge for ADR missions, the latest advances can be performed utilizing the existing advanced technology. Autonomous systems would be able to service the majority of space debris and end-of-life satellites using the same algorithms and methods [34].

In general terms, during absolute navigation, the main sensor to be used to reduce the orbital propagation error can be a GNSS receiver such as the Global Positioning System (GPS) used to obtain the position, typical sensors used for attitude control can be used in Attitude Determination.

To determine the relative state between the chaser and the target, different options are available:

- Vision-Based Navigation (VBN): The solution is obtained using optical devices. The relative position and attitude are determined individually, or both at the same time.
- Radar: The Time of Flight measurement of the emitted signal can quantify the range but not the relative position.
- Lidar: Light detection and ranging, same as radar, with extended ranges.

The main difficulty at the beginning of the closing phase lies in recognizing properly the target. The TLEs are of little help since their large cross-track error (up to a few hundred meters) does not significantly reduce the target search area in the image, so that many candidates can be simultaneously visible. Kinematic trajectory analysis is thus the preferred way for the target detection when initiating the approach, an algorithm such as the proposed in [35] can be used, which identifies a number of centroids of the objects acquired by the optical sensor, the algorithm needs first to collect a sequence of images to be able to detect a candidate

trajectory. An extra sensor for ranging like a Lidar would come into aid to identify the correct object.

During the relative navigation for close rendezvous, concerning position, velocities, attitude, and angular rates, the chaser is ready to start an inspection before initiating its deorbiting mission; this inspection may include a fly-around maneuver to acquire the approach axis.

Because of the increased navigation accuracy requirements, in many cases, a different type of sensor than in the previous phase has to be used for the final approach. In this case, toward the end of the closing phase, the acquisition conditions for the new sensor type have to be met. The rule of thumb is that the measurement accuracy must be of the order of 1% of range or better [36].

3.4.3 Pose estimation

Achieving reliable pose estimation of uncooperative satellites is a key technology for enabling IBS removal missions. The non-cooperative nature of the target becomes the real challenge that underlies pose estimation (the visual markers of attitude and distance), meanwhile, the inability to accomplish this goal can lead to the disruption in the deorbiting mission, forcing the SDO to tumble or rotate about the principal axis.

Attaining the goal of approaching close to the trajectory, requires a coherence relay between guidance and navigation. Navigation and estimation of the pose provide the framework to update guidance algorithms for the onboard generation of the approach trajectory. Previous literature has explored the introduction of a novel pose determination method based on Convolutional Neural Networks (CNN) to provide an initial guess of the pose in real-time on-board. The method involves discretizing the pose space and training the CNN with images corresponding to the resulting pose labels [37]. Since reliable training of the CNN requires massive image datasets and computational resources, the parameters of the CNN must be determined prior to the mission with synthetic imagery. Such a robust system requires reliable training of the CNN, combined with coherent datasets that appropriately account for noise, color, and illumination characteristics expected in orbit. Implementing a monocular camera ensures pose estimation under low power and low hardware complexity [38]. However, one caveat is that the monocular camera provides a clear image sequence limited by the observation condition. Therefore, it is necessary to study the pose estimate of the space object from a single image case. Existing computer vision methods rely on framing a prior shape model built based on the structural similarity of objects in a specific category, and the pose estimation of the unknown object that is reduced to a 3D-to-2D shape fitting problem where the parameters of shape and pose are estimated simultaneously. However, this logic is limited in the case of space objects, mainly due to the fact that the structure cannot be mapped similarly to commonly accessible objects like chairs or cars.

Considering the 3D pose of unknown space objects from a single image, noting that there are plenty of constraints among the components of typical space objects can be considered an alternative. From this, a hierarchical shape model of space objects can be proposed to describe the prior information of the object geometry, which represents the constraints among components of objects in the form of data gathered from the probability distribution. Therefore, with the support of the hierarchical shape model proposed, the pose estimation of unknown space objects can be conducted from a single image. To achieve mission objectives, the algorithms, including the navigation filter, for model-based, non-cooperative pose estimation using data from Lidar systems operate in the same frequency spectrum as range finders but are capable of creating 3D point clouds of scanned objects [39]. Multiple samples of a moving target using Lidar can provide enough information to perform the pose estimation of the target. Stereo cameras are capable of acquiring sparse 3D point cloud information similar to Lidar, although it requires a bit more processing. Data generated by camera sensors are more textured than Lidar scans. Lidar is more accurate over longer ranges and functionality. On the other hand, the range of stereo cameras is often limited by the baseline distance between the left- and right-hand cameras. Therefore, a couple of uses of both will be advantageous to the mission objectives. Non-cooperative pose estimation is performed using point cloud data generated by a series of Lidar images.

To develop a strong background for guidance inference from this knowledge, the dynamics model for proximity operations between a controlled chaser spacecraft and an uncontrolled target should be well-defined, considering that the model has path constraints required for safe maneuvering. Scans of satellite surfaces were matched with the known computer-aided design (CAD) models of the targets [39]. Shortcomings due to probable poor initial guess have been addressed in the reference [40] by implementing a novel clustered viewpoint feature histogram (CVFH) method.

From the existence of the state-of-the-art CNN, the model contains a local receptive field, which maps through the whole image to detect the features of the spacecraft. This detailed process converts the image pixels into numerical data by interpreting the attributes in the pixels with their respective local receptive field to correlate neurons of the first hidden layer. The information from these images is then passed through the layers of neurons until the pose at the final layer is determined. Trained CNN has the built-in ability to drive direct empirical correlation of the images and estimated poses. Finally, this solution is coupled with an EKF to perform the pose estimation of the target.

3.5 Stability and control of the deorbiting mission

Several studies have been published so far to study the attitude evolution, stability, and control of the SDO, Fig. 7 presents a diagram showing the evolution of the approaches.

The work in [41] creates the first 3-D numerical assessment and simulations of the IBS relative dynamics and control problem with the Ion Beam Interactor Simulator (IBIS), the equations of motion are implemented for two types of debris, spherical and cylindrical; a three-axis Proportional Derivative (PD) controller on the shepherd satellite is used to provide stable relative motion for both types of target debris while the problem of the debris attitude stability and control was not studied.

To study the motion of the debris due to the ion beam begins with the proposition of models to describe the distribution of an ion plume: the optimization and testing issues of ion beam thrusters for an IBS mission were addressed in Refs. [42, 43], the evolution of the quasi-neutral plasma plume sufficiently far from the thruster (far-field region) can be approximated with a self-similar fluid model that hinges on two main parameters, namely the upstream beam divergence angle and the plasma Mach number. In practice, the radius of a section containing 95% of the total current of the beam is commonly taken as the local width of the beam. State-of-the-art ion engines can be as low as 10–15 degrees.

Regarding the interaction of the ion beam with an SDO, the authors of Refs [14, 44, 45] developed simplified algorithms for determining the forces transmitted by an ion beam using the central projection of the SDO. More detailed results from experimental studies of the prolonged exposure of the ion beam on an object are described in [46], and expressions are derived for setting up a correspondence between the conditions of accelerated laboratory tests and the conditions of long-term exposure of an SDO to a plasma beam, modeled as on Earth's ionosphere.

The ion beam interaction with the SDO attitude dynamics and control during contactless de-orbiting is included in [47], the main simplifying assumption is that the relative position between the debris and the shepherd center of mass can be estimated at all times with no error. Semi-analytical relations were provided to be used for the evaluation of the beam force transmitted to a spherical target in a generic position with respect to a conical beam. Modified beam-perturbed CW equations in circular orbits for the relative motion of the SS-SDO system were derived. Finally, to attain the goal of contactless de-orbiting, the stability of the relative motion was investigated, the relative dynamics are unstable, in the open-loop case the beam action further destabilizes the maneuvers.

The studies in Refs. [48, 49] focus on the dynamics of a solid under the influence of ion flow and gravitational momentum. For the case of plane motion, a comparison of the descent times in different motion modes was carried out. It is also discovered that in low Earth orbits, the atmosphere begins to exert a significant influence. Additionally, it was shown that the motion of the space debris around its center of mass has a significant effect on its removal time. In addition, in [50] another important factor that influences the motion of a body is mentioned, at a given altitude the effect of the atmosphere is significant, a rough estimation shows that for a body on a circular orbit of 250 km altitude, the magnitude of the drag force is comparable to the force created by the ion flow.

Relative control of the IBS formation based on conventional approaches is studied in Refs. [47, 51, 52]. These papers assume that the spacecraft has high impulse thrusters that allow the control system to apply forces in orthogonal directions, the low specific impulse (Isp) thrusters are used to provide the stability and performance of the relative motion. However, a low Isp of such thrusters together with a long-lasting de-orbiting phase reduces the economic attractiveness of the IBS concept and limits its multi-mission capabilities. This feature and the duration of the de-orbiting phase imply that the mass of propellant to control the Shepherd relative position can result in an important share of the total propellant consumption of the mission.
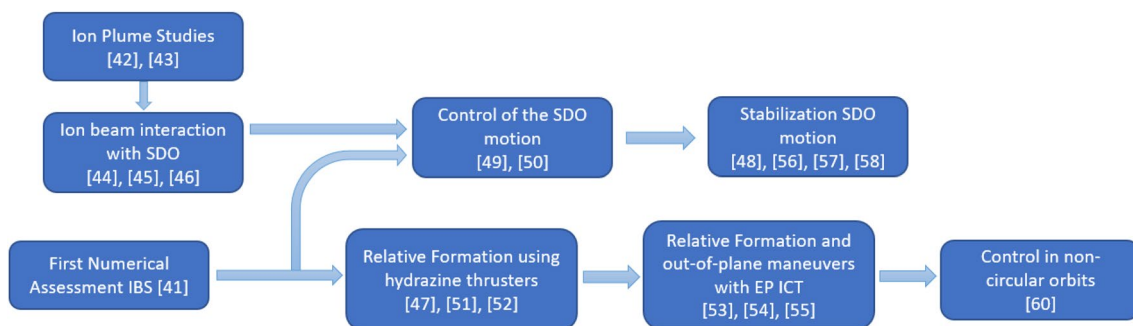

Fig. 7 Diagram of the advances in control techniques for the IBS mission

A different control strategy presented in [53] focuses on the reduction of the propellant consumption by maximizing the de-orbiting rate of the SDO; it is achieved by maintaining a maximum magnitude ITT thrust. At the same time, the thrust of the ICT can be adjusted to control the relative motion of the SS. Furthermore, to minimize propellant consumption, Ref. [54] suggested using a small variation of the thrust in the ICT to keep the in-plane relative position of the SS between certain boundaries. The results of Ref. [55] expand the capabilities of this approach, by applying the strategy to the out-of-plane relative position of the SS, it is shown that the spatial relative position requirement for the formation can be controlled by varying two main values: the yaw angle of the SS and thrust of the ICT; This strategy simplifies the architecture of the control system while reducing its cost, and saving propellant. A problem with this approach is that it can maintain the required relative position of the underactuated SS with a periodic error; this is a minimum problem when the orbits have very low eccentricity, but this error grows as eccentricity increases which could lead to problems for debris objects in high eccentric orbits that need to be removed.

Previous research have shown that an object's attitude motion has a significant impact on the efficiency of the ion beam transportation process [48], in [56] an unperturbed motion of the system in a circular orbit is studied, two cases of descent of space debris were compared, calculations have shown that the time difference in time spent on descent with and without SDO attitude control motion can be significative. At the same time, the saving of fuel spent on the spacecraft position control is around 16% for engines.

In [57, 58] a control law for 3D motion of an SDO is considered, the aim was to provide stabilization of the object oscillations in an equilibrium state. It is proposed to change the thrust of the ion engine to change the orientation of the passive object. When applying the force to a cylindrical target, it is found that the orientation of the cylindrical object, corresponding to the maximum value of the force generated by the ion beam, does not coincide with stable equilibrium positions. To keep the object in this position, additional efforts are required. A phase trajectory on which the average ion beam force is maximum in absolute value was determined.

Finally, the dissertation [59] addresses the problem of relative motion control in eccentric orbits using methods of robust control theory, but here, like in Ref. [48], is assumed that there is a set of multiple thrusters, which applies control actions in all orthogonal directions. To use only EP, the reference [60] focuses on debris removal methods in noncircular (eccentric) orbit, the research investigated the viability of using a single IC to control the relative position of the ion-beam shepherd in eccentric orbits. Two controllers were used for the shepherd satellite: a time-invariant and periodic linear-quadratic regulator. Both maintain the relative position of the shepherd with periodic errors, which grow as orbital eccentricity increases, a problem similar to the one found in [55]. The controller can be designed with a periodic reference input to reduce the relative position errors and improve the efficiency of the ion momentum transmission.

The final steps to consolidate the strategies for control of an IBS deorbiting mission are related to the implementation of robust control techniques that include conditions, to name a few: non-ideal estimation of the target's relative position and orientation, the influence of eclipses in sensors, optimal solutions minimizing propellant consumption, non-rigid body dynamics control techniques of the stability of the SS due to its large solar arrays, etc.

4 Architecture of the IBS

It is important to note that even if the studies and research about the IBS have been appearing continuously in conferences and journals, until the date of the writing of this manuscript, no formal mission proposal using the IBS concept has been presented yet. There could be several reasons for this, including the low TRL of some of the key technologies.

This section aims to review the architecture for an IBS mission and find the missing links for a demonstration mission. The main aspects analyzed are the necessary propulsion system and platform design for the Ion Beam Shepherd mission. The propulsion subsection reviews the available suitable choices of thruster engines and comparative analysis among them. The platform subsection reviews graphical analysis of time, specific impulse, mass, and power with respect to thrust force to deorbit target debris.

4.1 Propulsion

Some of the design considerations that have been made for the IBS missions, keeping in mind earlier research, are as follows:

  i. Improved thruster performance by reducing thruster power and efficient utilization of mass
 ii. Decreased thruster mass suitable for a small shepherd satellite (<500 kg)
iii. Higher thrust force and large thrust time
 iv. Increased Isp during deorbiting debris for faster maneuverability
  v. Highly converged ion beam for efficient irradiation

Among all the available electrical propulsion technologies, the electrothermal propulsion type including resistojets

and arcjets provide extremely low impulse (Isp), and low propellant efficiency compared to the other two varieties which are electrostatic and electromagnetic thrusters. Among these, electrostatic gridded ion thrusters (GIE), hall thrusters (HET) and Stationary Plasma Thrusters (SPT) have been identified as the best suitable choices due to their high efficiency and higher specific impulse.

An analysis of some of these thrusters based on their performance attributes is presented in Table 1. The SPT-140 provides maximum thrust and has minimum mass [61]. The HiPeP thruster provides a very large Isp but its power consumption is unreasonably large [62]. Even though the CAMILA-HET has minimum power consumption it provides a really less thrust force and has lesser efficiency as compared to the NEXT thruster which has maximum efficiency and the T6 thruster which provides very high Isp [63, 65]. The T7 thruster on the other hand provides higher efficiency and Isp compared to T6, yet it has a larger mass and a TRL of 5 [65].

Another concept that has proved to be promising is the Double-Sided Ion thruster (DST), gradually shaping from a mere idea to demonstrated technology within a span of a few years [66]. Some of its advantages include simpler subsystem architecture, lower cost, lower total mass, and half RF power compared to two single-ended thrusters. In [67], the thruster was designed where power and low beam divergent requirements were identified. A model was developed to predict its performance and using this model design parameters such as size, ion optics geometry, and beam voltage of the thruster were determined. The advancement in [68] dealt with the optimization of EP in IBS, which made it possible to identify optimal operating points of both ITT and ICT individually [64, 69]. It was found that minimizing either total dedicated mass or total thruster power for two different beam voltages of the two thrusters was needed, depending on the mission specifications. It was also studied that beam expansion majorly reduces momentum transfer to the target object, which in turn affects the efficiency of IBS technique. In addition, there could be a reduction in the increase of beam divergence by a high operational voltage.

The authors felt it was wise to investigate different technology thrusters, specifically HET for ICTs since it has a better thrust-to-power ratio compared to ion thrusters [53]. Later, there was an experimental campaign that displayed promising results regarding the double-sided thruster. Four different configurations were tested namely: Active IT Beam (AIT) with inactive IC, Active IC Beam (AIC) with inactive IT, Active Double-sided thruster (ADST) with only one grid as part of IT ion optics system, and ADST with screen grids located at each ion optics side, the thruster operated in double-sided mode with both sides of thrusters active. A comparative analysis was studied for all the configurations [68]. Results showed that the IT:IC thrust ratio depends on three factors which are screen grid voltage, Radio Frequency Generator power, and mass flow rate. In fact, to achieve IT and IC thrust force, accel voltage is required to be changed. It was also possible to extract two ion beams from the same discharge chamber such that the IC ion optics side generated approximately 30% more thrust compared to IT [59]. Currently, the TRL is 5 for DST, however, further system prototype demonstration in space could make it one of the future absolute choices for IBS missions.

4.2 Platform

The work in [14] presents a preliminary design methodology for an IBS mission, it is based on determining design and operational constraints that can be achieved by a feasible solution. Ultimately, there are two main constraints that define the possible mission: the separation distance with respect to the SDO to be deorbited, and the thrust level. It is desirable to keep the separation distance as short as possible, to maximize the level of thrust and minimize the time of deorbiting while keeping a too close distance could result in back sputtering contamination effects and increased risk of collisions. On the other hand, high values of thrust increase the back sputtering and also the power consumption requirements, which would increase the mass of the satellite.

Table 1 Comparison of main characteristics of Electric Propulsion thrusters: Technology, power, Isp, thrust, mass, TRL

EP technology	Thruster name	Power [W]	Isp [s]	η [%]	Thrust [mN]	Mass [kg]	TRL
GIE	XIPS (25 cm)	4200	3800	67	165	13.7	9
GIE	T6	5000	>4000	68	30–230	31	9
GIE	T7	7000	>4000	NA	Up to 290	13	5
GIE	NEXT	6900	4190	70	236	52	9
Xe Ion engines via microwaves	HiPEP	30,000	8900	80	540	Very high	9
Hall Effect Thrusters	CAMILA-HET	250	1570 ± 73	43 ± 3.7	13.9 ± 0.6	<12	9
Stationary Plasma Thruster	SPT-70	700	1500	45	40	1.5	9
Double Sided Ion Thruster	DST (IT & IC)	416	1545	18.5	IT: 3.6, IC: 6.5	10.6	5

From the point of view of cost limitations, a demonstration mission for the IBS would most likely be feasible within a small satellite form factor, therefore, the companion software application [70] developed in [14] is taken as a reference to estimate the sizing of a small feasible IBS spacecraft. The input parameters are described in Table 2, unlike other references cited before, the target is set to be a small debris object, not exceeding 200 kg, a larger target would necessarily result in a bigger SS. The initial orbit has an altitude of 700 km for the reasons explained in Sect. 3.2, the thruster and plasma parameters were selected to coincide with the Stationary Plasma Thruster. The constraints indicate that the distance from the target will be between the range of 9 to 23 m, the lifetime of the mission has to be below 150 days, with a worst-case Momentum Transfer Efficiency (ηB) of 0.15. A Reaction Control System (RCS) is included in the platform for approaching maneuvers and possible momentum unloading.

The results seen in Fig. 8 show a feasible space of solutions with the selected input parameters, according to different combinations of separation distance and thruster force, the deorbiting time is expected to be around 60–90 days, it is noticeable that the power needs are very demanding, the required power consumption can be as high as close to 2.3 kW, which could result in disproportionately large solar arrays for a small platform.

5 Additional considerations and other risks

This section describes the additional risks and considerations that are evident in the IBS method.

5.1 Backflow contamination

As a result of the interaction of the incoming beam with the outgoing ions and neutrals from the debris backscattered, the intrusion of a debris body in the plasma plume may complicate the satellite environment. This environment can affect negatively the performance of the IBS subsystems through various interactions: the appearance of parasitic currents on biased surfaces, degradation of solar array panels, thermal control, and other surfaces, or attenuation and refraction of electromagnetic wave transmission and reception due to the enhanced plasma density.

The use of plasma thrusters involves backflow contamination risks by itself. The two most relevant processes are charge-exchange collisions (CEX) between ions and not-ionized propellant, which produce slow ions that might return onto the spacecraft if the radial electric field pushes them towards e.g. solar panels, and deposition of thruster material particles sputtered from thruster walls that can become charged. These hazards are normally accounted for in satellite design, mainly by skewing beam axes away from solar panels and other sensitive equipment at a certain angle, so that satellite life is not substantially affected [21].

However, for the IBS concept, it is important also to assess the formation of CEX ions due to collisions with the neutral xenon atoms returning from the debris, and the effect of incoming sputtered material. Xenon ions do not pose a serious contamination hazard for exposed satellite surfaces such as solar panels, although they might give rise to parasitic current flows between biased surfaces. A low-pressure cloud of neutral xenon gas and particles is expected to occur naturally around the debris surface irradiated by the ion beam thruster configuration. As they expand into the vacuum, these neutrals may give rise to CEX ions close to the debris surface [71].

Table 2 Parameters used for the design case of a small platform

| Target Body		Space Shepherd					
Mass	Equivalent radius	Mass SS	RCS propellant mass	Structure mass	PPU Conversion η	Platform power	Max power
200 kg	1 m	373 kg	15 kg	125 kg	0.9	500 W	2400 kW
Ion Thruster and Plasma Plume							
Max. Thrust	Min. Thrust	Max. Power	Min. Power	Isp range (min–max)		Thruster ηT	Divergence angle
40 mN	20 mN	1 kW	450 W	2000s	2500 s	0.45	15 deg
Orbit				Constraints			
Initial altitude	Final altitude	Eclipse fraction	Drag coeff	Collision avoidance	Sensor sensitivity	Max. lifetime	Min. MTB ηB
700 km	500 km	0.38	2.2	9 m	23 m	150 days	0.15
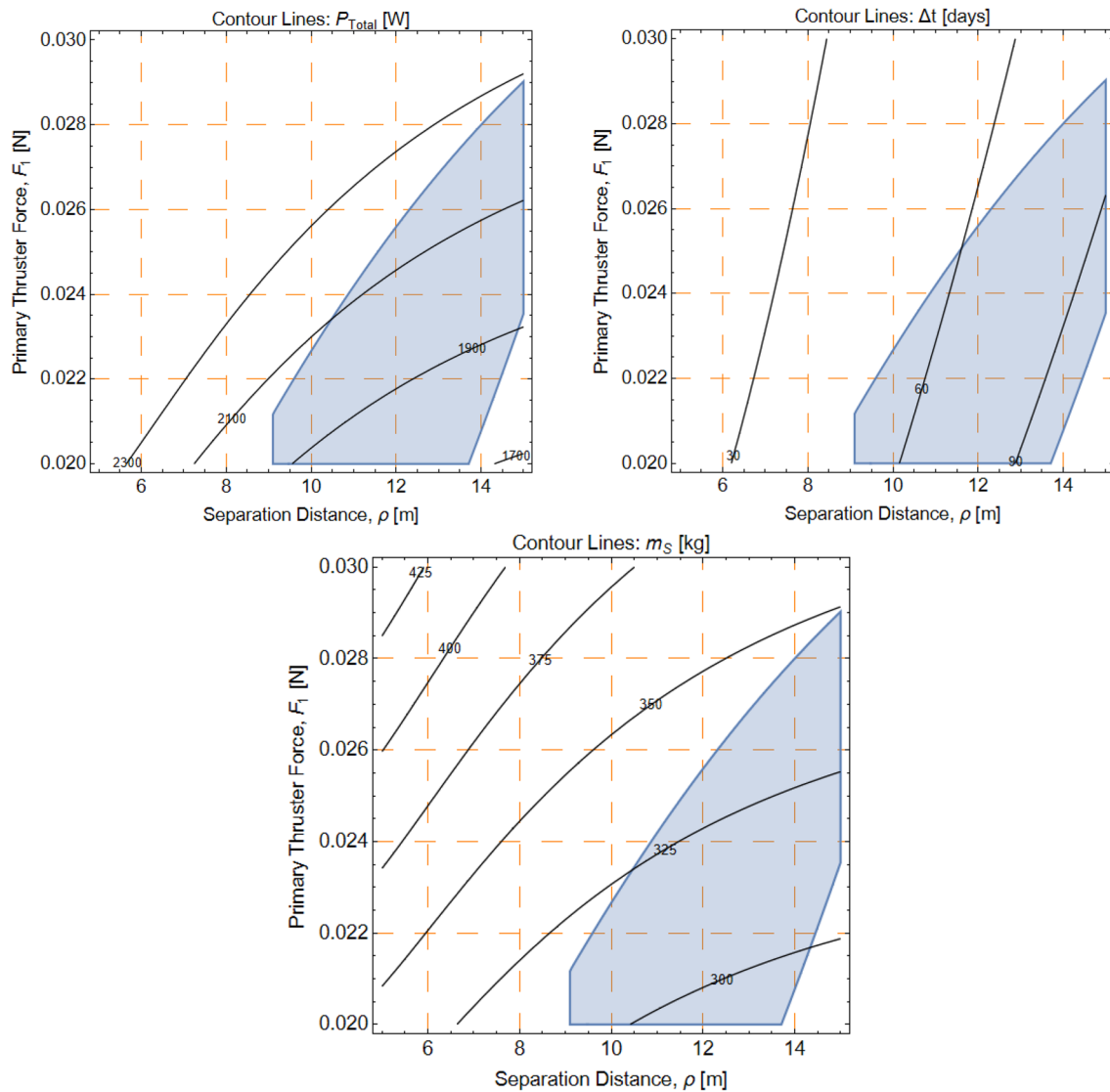
Fig.8 Design envelop including contour lines for constant values of total power (top left), deorbiting time (top right), and total mass of spacecraft (bottom)

Detailed quantification of the importance of this effect requires knowledge of the neutral density. However, it can be anticipated that for an IBS acting on debris sufficiently far from the IBS, ion densities near the surface are low enough to neglect the formation of CEX ions.

Due to the larger distances being considered, most CEX ions occurring far downstream in the plume are expected to be pushed away radially with an angle large enough from the centerline as to not come back upon the satellite, additionally, plasma sheath electric potential might be beneficial as it pulls those ions and hinders their back streaming. Assuming a spherical expansion from the surface of a sphere of approximately 1 m radius, sputtered material flux would be about 100 times lower when it reaches the IBS (at ~ 10 m distance from the debris) [72].

Assessment of the effects of this flux on the IBS lifetime requires improving this coarse estimate and detailed study of particle–surface interactions close to the structural interface of the IBS. To summarize, the effect of back sputtering is a risk that can be considered in the mission, however, the effect of it is not threatening the longevity and purpose of mission objectives.

5.2 Torque due to misalignment of thrust and center of mass

If the resultant thrust force produced by the ITT and the ICT is misaligned with the center of mass, this thruster force vector misalignment causes a moment around the center of mass of the satellite during thruster operation. If

this disturbance moment is not adequately rejected by the satellite control system, it could cause significant errors when precise maneuvering is required, for example during satellite maneuvering when in close proximity to another satellite. This disturbance torque problem is mentioned in [73], it is proposed the use of reaction jets, gimballing the thruster nozzle, off-modulating a multi-thruster system. This is possible for the IBS given that the IBS includes an RCS, which has a limited amount of propellant to use. An alternative would be to use reaction wheels to compensate for the moment, but the disadvantage is the build-up momentum in the reaction wheels that needs to be dumped by using another actuator like a magnetic torquer.

To evaluate the best solution, it is of foremost importance to estimate the thruster force response characteristic with a sufficient degree of accuracy. The work in [75] describes the roll torque produced by NASA's Evolutionary Xenon Thruster (NEXT) ion thruster through a combination of theoretical calculations and magnetic field simulations. In Ion thrusters, not only the mechanical misalignment of the thrusters can produce an off-axis force, the nature of the ions flowing through grids and the presence of magnetic field lines can create thrust misalignment errors, more precisely, the possible sources of error are:

- Beamlet Deflection Due to Grid Misalignment.
- Magnetic Field Produced Torque due to the ions subject to the Lorentz force.
- Placement of the neutralizer cathode, although usually dismissed in comparison with the previous ones.

Theory calculations and measurements of the disturbance torques are presented in [74], the ion thrusters produce a roll torque about the thrust axis due to both rotational grid misalignments and the magnetic field that leaks out into the plume. This effect is non-negligible and must be considered as a potential risk in Ion Beam thrusters. The past experience of Ion Thruster missions utilizing ion thrusters was mentioned, these missions utilized hydrazine to counteract the ion thruster produced roll torque, and some missions were ended when the onboard hydrazine was depleted, such is the case of the Dawn mission, the roll torque estimated prior to launch was less than the actual roll torque observed in flight. However, the clocking misalignment measurements correctly predicted the directions of roll torque. Therefore, a more convenient method to mitigate this risk would be measuring roll torque before launching it, using an electrostatic probe that will coincide qualitatively with thrust vector measurements made on the same thruster, therefore predicting the effects of this torque. This ultimately allows

sizing the actuators accordingly with their respective moment unloading techniques.

6 Conclusions

Every new technology comes with certain benefits and challenges. Some of the benefits of IBS are: (a) it is applicable to the removal of multiple target debris, (b) this technology works irrespective of the size, shape, material, or its rotational state, (c) it is reusable technology unless fuel is completely depletion, (d) it has no necessity of docking which makes it a contactless technology, (e) it is cost-effective, and (f) has future prospects like transportation, space mobility, in-orbit assembly of large infrastructures.

This technology can operate only in close range due to beam divergence effects and pointing errors. The momentum transfer concept is ineffective considering the mass of the debris and the thrust produced. Collision avoidance, sputtering of the debris and the backflow of Ions are the biggest challenges of the IBS method. The fallout from the plasma plume interaction between the spacecraft and the debris also adds to the challenges of using IBS. In spite of these challenges, years of study and investigation have shown that if organizations could work towards developing it and increasing the TRL, it could be one of the most promising and efficient long-term solutions to this persistent problem of space debris.

7 Copyright Statement

Declarations

References

1. Virgili Llop, J., Drew, J., Zappulla, R., & Romano, M.: Autonomous capture of a resident space object by a spacecraft with a robotic manipulator: Analysis, simulation and experiments. In AIAA/AAS astrodynamics specialist conference (p. 5269). (2016). https://doi.org/10.2514/6.2016-5269

2. Gangapersaud, R.A., Liu, G., de Ruiter, A.H.: Detumbling a non-cooperative space target with model uncertainties using a space manipulator. J. Guid. Control. Dyn. **42**(4), 910–918 (2019). https://doi.org/10.2514/1.G003111

3. Dong, H.A.N., Gangqi, D.O.N.G., Huang, P., Zhiqing, M.A.: Capture and detumbling control for active debris removal by a dual-arm space robot. Chinese J. Aeronaut. (2021). https://doi.org/10.1016/j.cja.2021.10.008

4. Sánchez-Arriaga, G., Castellani, L. T., Lorenzini, E. C., Tajmar, M., Wätzig, K., & Post, A.: Status of development of a deorbit device based on electrodynamic tether technology in the ET PACK Project. In proceedings of 8th European conference on space debris (virtual edition, SDC8). (2021). https://conference.sdo.esoc.esa.int/proceedings/sdc8/paper/96

5. Matsumoto, K., Shiomi, H., Kawamoto, S., Ohkawa, Y., Iki, K., & Takahashi, A.: Mechanisms and lubrication of electrodynamic tether system for debris removal. In European space mechanisms & tribology symposium. (2013). (pp. 25–27)

6. Ohkawa, Y., Kawamoto, S., Higashide, M., Iki, K., Baba, M., Kitamura, S., & Kibe, S.: Electrodynamic tether propulsion for orbital debris deorbit. J. Space Technol. Sci. 26(1), 1_33–1_46. (2012). https://www.jstage.jst.go.jp/article/jsts/26/1/26_1_33/_pdf

7. Senwei, L. V., Haojun Zhang., Yao Zhang., Bowen Ning.: Rui Qi 2. Design of an integrated platform for active debris removal. Aerospace 9, 339. (2022). https://doi.org/10.3390/aerospace9070339

8. Stadny, K., Hovell, K., Brewster, L.: Space debris removal with sub-tethered net: a feasibility study and preliminary design. Proc. 8th European Conference on Space Debris (virtual), Darmstadt, Germany, 20–23 April (2021)

9. Eleonora, M., Botta, Inna Sharf., Arun Misra.: Tether-nets for active space debris removal: Effect of the tether on deployment and capture dynamics. https://escholarship.mcgill.ca/concern/theses/rv042w43j

10. Minghe Shan., JianGuo., Eberhard Gill.: Review and comparison of active space debris capturing and removal methods. https://doi.org/10.1016/j.paerosci.2015.11.001

11. Jaime Reed.L.: Simon barraclough. Development of harpoon system for capturing space debris. Proc. '6th European conference on space debris' Darmstadt, Germany, (2013)

12. Shen Shuangyan., Jin Xing., Chang Hao.: Cleaning space debris with a space-based laser system. http://dx.doi.org/https://doi.org/10.1016/j.cja.2014.05.002

13. Priyant Mark, C., Surekha Kamath.: Review of active space debris removal methods. https://doi.org/10.1016/j.spacepol.2018.12.005

14. Urrutxua, H., Bombardelli, C., Hedo, J.M.: A preliminary design procedure for an ion-beam shepherd mission. Aerosp. Sci. Technol. **88**, 421–435 (2019). https://doi.org/10.1016/j.ast.2019.03.038

15. Jason Forshaw., Guglielmo Aglietti., Simon Fellowes., Thierry Salmon., Ingo Retat., Alexander Hall., Thomas Chabot., Aurélien Pisseloup., Daniel Tye., Cesar Bernal., et al. The active space debris removal mission RemoveDebris, Part 1: from concept to launch. https://hal.inria.fr/hal-02286651

16. Aglietti, G.S., Taylor, S., Fellowes, S., Salmon, T., Retat, I., Hall, A., Chabot, T., Pisseloup, A., Cox, C., Zarkesh, A., Mafficini, A., Vinkoff, N., Bashford, K., Bernal, C., Chaumette, F., Pollini, A., Steyn, W.H.: The active space debris removal mission RemoveDebris. Part 2: in orbit operations, Acta Astronautica, https://doi.org/10.1016/j.actaastro.2019.09.001

17. Gene Fujii., Seita Iizuka., Carolyn Belle., Mark Muktoyuk.: The World's first commercial debris removal demonstration mission, 35th annual small satellite conference. https://digitalcommons.usu.edu/smallsat/2021/all2021/145/

18. Richard, M., Kronig, L., Belloni, F., Rossi, S., Gass, V., Araomi, S., Gavrilovich, I., Shea, H., Paccolat, C., Thiran, J. P.: Uncooperative rendezvous and docking for microsats1. Presented at the 6th international conference on recent advances in space technologies, RAST 2013, 12–14, Istanbul, Türkiye (2013)

19. Diego Escorial Olmos., Thomas Vincent Peters., Joris Naudet., Cristian Corneliu Chitu., Karol Sewerin., Tomasz Barciński.: Android small active debris removal mission. Challenges in European aerospace, 5th CEAS Air and Space Conference

20. Oda, Mitsushige.: ETS-VII: Achievements, troubles and future. Proceeding of the 6th international symposium on artificial intelligence and robotics & automation in space: i-SAIRAS 2001, Canadian space agency, St-Hubert, Quebec, Canada, 18–22 June (2001)

21. Bombardelli, C., Pelaez, J.: Ion beam shepherd for contactless space debris removal. J. Guid. Control. Dyn. **34**(3), 916–920 (2011). https://doi.org/10.2514/1.51832

22. Union of concerned satellites, "UCS satellite database" Published Dec 8, 2005, https://www.ucsusa.org/resources/satellite-database (Accessed 10.10.21)

23. Clohessy, W.H., Wiltshire, R.S.: Terminal guidance system for satellite rendezvous. J. Aerospace Sci. **27**(9), 653–658 (1960). https://doi.org/10.2514/8.8704

24. Dana-Bashian, D., Hablani, H., & Tapper, M.: Guidance algorithms for autonomous rendezvous of spacecraft with a target vehicle in circular orbit. In AIAA Guidance, Navigation, and control conference and Exhibit (p. 4393), (2001)

25. Breger, L., How, J.P.: Safe trajectories for autonomous rendezvous of spacecraft. J. Guid. Control. Dyn. **31**(5), 1478–1489 (2008). https://doi.org/10.2514/1.29590

26. Rawlings, J.B., Mayne, D.Q., Diehl, M.: Model predictive control: theory, computation, and design, vol. 2. Nob Hill Publishing, Madison (2017)

27. LaValle, S.M.: Rapidly-exploring random trees: a new tool for path planning. The annual research report (1998)

28. Wilde, M., Ciarcià, M., Grompone, A., Romano, M.: Experimental characterization of inverse dynamics guidance in docking with a rotating target. J. Guid. Control. Dyn. **39**(6), 1173–1187 (2016)

29. Cabrales Hernandez, A. D.: Real-time quasi-analytical trajectory generation for docking with tumbling objects (Doctoral dissertation, Massachusetts Institute of Technology) (2020)

30. Garcia, A., Dawson, C., Lifson, M., Arnas, D., Fan, C., Jewison, C., & Linares, R. Model predictive control and safety analysis for satellite collision avoidance.

31. Ventura, J.: Autonomous proximity operations for noncooperative space targets (Doctoral dissertation, Technische Universität München) (2016)

32. Cabrales Hernandez, A. D.: Real-time quasi-analytical trajectory generation for docking with tumbling objects (Doctoral dissertation, Massachusetts Institute of Technology) (2020)

33. Silvestrini, S., Prinetto, J., Zanotti, G., & Lavagna, M.: Design of robust passively safe relative trajectories for uncooperative debris imaging in preparation to removal. In 2020 AAS/AIAA astrodynamics specialist conference (pp. 1–18) (2020)

34. Ventura, J.: Autonomous proximity operations for noncooperative space targets (Doctoral dissertation, Technische Universität München) (2016)

35. Ardaens, J.S., Gaias, G.: Flight demonstration of spaceborne real-time angles-only navigation to a noncooperative target in

low earth orbit. Acta Astronaut. **153**, 367–382 (2018). https://doi.org/10.1016/j.actaastro.2018.01.044

36. Fehse, W.: Automated rendezvous and docking of spacecraft. Cambridge university press. vol.16 (2003) https://doi.org/10.1017/CBO9780511543388.008

37. Sharma, S., Beierle, C., & D'Amico, S.: Pose estimation for non-cooperative spacecraft rendezvous using convolutional neural networks. In 2018 IEEE aerospace conference (pp. 1–12). IEEE. (2018). https://doi.org/10.1109/AERO.2018.8396425

38. Ren, X., Jiang, L., Wang, Z.: Pose estimation of uncooperative unknown space objects from a single image. Int. J. Aerospace Eng. (2020). https://doi.org/10.1155/2020/9966311

39. De Jongh W.C.: Space debris: pose estimation using stereo vision (Doctoral dissertation, Stellenbosch: Stellenbosch University). (2019)

40. Woods, J.O., Christian, J.A.: Lidar-based relative navigation with respect to non-cooperative objects. Acta Astronaut. **126**, 298–311 (2016). https://doi.org/10.1016/j.actaastro.2016.05.007

41. Bombardelli, C., Ahedo, M., Merino, E., Pelaez, J., Summerer, L., Urrutxua, H.: Space debris removal with an ion beam shepherd satellite: Dynamics and control. In proceedings of the 62nd international astronautical congress, Cape Town, South Africa. (2011)

42. Ahedo, E., Merino, M., Bombardelli, C., Urrutxua, H., Pelaez, J., Summerer, L.: Space debris removal with an ion beam shepherd satellite: target-plasma interaction. In 47th AIAA/ASME/SAE/ASEE joint propulsion conference & exhibit (p. 6142). (2011). https://doi.org/10.2514/6.2011-6142

43. Merino, M., Cichocki, F., Ahedo, E.: A collisionless plasma thruster plume expansion model. Plasma Sources Sci. Technol. **24**(3), 035006 (2015)

44. Alpatov, A. P., Fokov, A., Khoroshylov, S., Cichocki, A., Merino, M., Zakrzhevski, A.: IAC-15-A6. 5.5 Algorithm for determination of force transmitted by flume of ion thruster to orbital object using photo camera. In proceedings of the international astronautical congress, IAC (pp. 2239–2247). (2015)

45. Alpatov, A., Cichocki, F., Fokov, A., Khoroshylov, S., Merino, M., Zakrzhevskii, A.: Determination of the force transmitted by an ion thruster plasma plume to an orbital object. Acta Astronaut. **119**, 241–251 (2016). https://doi.org/10.1016/j.actaastro.2015.11.020

46. Shuvalov, V.A., Gorev, N.B., Tokmak, N.A., Kochubei, G.S.: Physical simulation of the long-term dynamic action of a plasma beam on a space debris object. Acta Astronaut. **132**, 97–102 (2017). https://doi.org/10.1016/j.actaastro.2016.11.039

47. Bombardelli, C., Urrutxua, H., Merino, M., Ahedo, E., Peláez, J.: Relative dynamics and control of an ion beam shepherd satellite. Spaceflight Mechan **143**, 2145–2158 (2012)

48. Aslanov, V.S., Ledkov, A.S.: Attitude motion of cylindrical space debris during its removal by ion beam. Math. Probl. Eng. (2017). https://doi.org/10.1155/2017/1986374

49. Aslanov, V.S., Ledkov, A.S.: Space debris attitude control during contactless transportation in planar case. J. Guid. Control. Dyn. **43**(3), 451–461 (2020). https://doi.org/10.2514/1.G004686

50. Ledkov, A. S., Aslanov, V. S.: Attitude motion of space debris during its removal by ion beam taking into account atmospheric disturbance. J Phys Confer Series (Vol. 1050, No. 1, p. 012041). IOP Publishing. (2018) https://doi.org/10.1088/1742-6596/1050/1/012041

51. Khoroshylov, S.V.: Relative motion control system of spacecraft for contactless space debris removal. Sci. innov **14**(4), 5–16 (2018)

52. Alpatov, A.P., Khoroshylov, S.V., Maslova, A. I.: Contactless deorbiting of space debris by the ion beam. Dynam Control (2019) https://doi.org/10.15407/akademperiodyka.383.170

53. Cichocki, F., Merino, M., Ahedo, E., Smirnova, M., Mingo, A., Dobkevicius, M.: Electric propulsion subsystem optimization for "Ion Beam Shepherd" missions. J. Propul. Power **33**(2), 370–378 (2017). https://doi.org/10.2514/1.B36105

54. Alpatov, A., Khoroshylov, S., Bombardelli, C.: Relative control of an ion beam shepherd satellite using the impulse compensation thruster. Acta Astronaut. **151**, 543–554 (2018). https://doi.org/10.1016/j.actaastro.2018.06.056

55. Khoroshylov, S.: Out-of-plane relative control of an ion beam shepherd satellite using yaw attitude deviations. Acta Astronaut. **164**, 254–261 (2019). https://doi.org/10.1016/j.actaastro.2019.08.016

56. Popov, G. A., Aslanov, V. S., Petukhov, V., Ledkov, A. Influence of space debris attitude motion on ion beam assisted removal mission costs, IAC-20, B4,6B,08, International Astronautical Congress 2020, online edition (2020)

57. Aslanov, V.S., Ledkov, A.S.: Dynamics and control of space debris during its contactless ion beam assisted removal. J Phys Confer Series IOP Publishing **1705**(1), 012006 (2020). https://doi.org/10.1088/1742-6596/1705/1/012006

58. Aslanov, V. S., Popov, G. A., Petukhov, V., Ledkov, A.: Attitude dynamics and control of space object during contactless transportation by ion beam. In IAC-20,A6,6,8,x56928 International Astronautical Congress 2020, online edition. (2020)

59. Ankersen, F.: Guidance, navigation, control and relative dynamics for spacecraft proximity maneuvers. (2010)

60. Khoroshylov, S.: Relative control of an ion beam shepherd satellite in eccentric orbits. Acta Astronaut. **176**, 89–98 (2020). https://doi.org/10.1016/j.actaastro.2020.06.027

61. Garner, C. E., Jorns, B., Hofer, R. R., Liang, R., & Delgado, J.: Low-power operation and plasma characterization of a qualification model SPT-140 hall thruster. In 51st AIAA/SAE/ASEE Joint Propulsion Conference (p. 3720). (2015) https://doi.org/10.2514/6.2015-3720

62. Foster, J., Haag, T., Kamhawi, H., Patterson, M., Malone, S., & Elliot, F.: The high power electric propulsion (HiPEP) ion thruster. In 40th AIAA/ASME/SAE/ASEE joint propulsion conference and exhibit (p. 3812). (2004) https://doi.org/10.2514/6.2004-3812

63. Szabo, J. J., Pote, B., Tedrake, R., Paintal, S., Byrne, L., Hruby, V. J., & Smith, T. High throughput 600 watt Hall effect thruster for space exploration. In 52nd AIAA/SAE/ASEE Joint Propulsion Conference (p. 4830). (2016). https://doi.org/10.2514/6.2016-4830

64. Fisher, J.: NEXT-C Flight ion system status. In AIAA propulsion and energy 2020 Forum (p. 3604). (2020) https://doi.org/10.2514/6.2020-3604

65. Luna, J. P., Lewis, R. A., Park, N., Bosher, J., Guarducci, F., & Cannat, F.: T7 thruster design and performance. (2019)

66. Kitamura, S., Hayakawa, Y., Kawamoto, S.: A reorbiter for large GEO debris objects using ion beam irradiation. Acta Astronaut. **94**(2), 725–735 (2014). https://doi.org/10.1016/j.actaastro.2013.07.037

67. Feili, D., Ruiz, M., Merino, M., Cichocki, F., Ahedo, E., Smirnova, M., & Dobkevicius, M.: Impulse transfer thruster for an ion beam shepherd mission. In 34th international electric propulsion conference, IEPC-382. (2015)

68. Dobkevicius, M., Smirnova, M., Perez, A. M., & Feili, D.: Double-sided ion thruster for contactless space debris removal: experimental results. In 35th international electric propulsion conference, IEPC-2017–261. (2017)

69. Dobkevicius, M., Feili, D., Smirnova, M., Perez, A.M.: Design and testing of a double-sided ion thruster for ion-beam shepherd. J. Propul. Power **36**(2), 202–210 (2020). https://doi.org/10.2514/1.B37380

70. IBS Design companion software application in a Mathematica interactive computable document format under the GNU GPL

v3 License. http://sdg.aero.upm.es/ONLINEAPPS/IBS_Design (Accessed 10.10.21).

71. Shan, M., Guo, J., Gill, E.: Review and comparison of active space debris capturing and removal methods. Prog. Aerosp. Sci. **80**, 18–32 (2016). https://doi.org/10.1016/j.paerosci.2015.11.001

72. Myers, R., Arrington, L., Pencil, E., Carter, J., Heminger, J., & Gatsonis, N.: Pulsed plasma thruster contamination. In 32nd joint propulsion conference and exhibit (p. 2729). (1996) https://doi.org/10.2514/6.1996-2729

73. Bryson, A.E.: Control of spacecraft and aircraft, vol. 41. Princeton University Press, Princeton (1993)

74. Arthur, N. A.: Ion thruster produced roll torque. In AIAA propulsion and energy 2019 Forum (p. 4166). (2019)